

Excitation spectra and spin gap of the half-filled Holstein-Hubbard model

Martin Hohenadler and Fakher F. Assaad

Institut für Theoretische Physik und Astrophysik, Universität Würzburg, 97074 Würzburg, Germany

(Dated: March 1, 2013)

Single- and two-particle excitation spectra of the one-dimensional, half-filled Holstein-Hubbard model are calculated using the continuous-time quantum Monte Carlo method. In the metallic phase, the results are consistent with a Luther-Emery liquid that has gapped spin and single-particle excitations but a gapless charge mode. However, given the initially exponential dependence of the spin gap on the backscattering matrix element, the numerical excitation spectra appear gapless in the weak-coupling regime, and therefore resemble those of a Luttinger liquid. The Mott phase has the expected charge gap and gapless spin excitations. The Peierls state shows a charge, spin and single-particle gap, a soft phonon mode, backfolded shadow bands and soliton excitations. Arguments and numerical evidence for the existence of a nonzero spin gap throughout the metallic phase are provided in terms of equal-time spin and charge correlation functions.

PACS numbers: 71.10.Hf, 71.10.Pm, 71.45.Lr, 71.30.+h, 71.38.-k

I. INTRODUCTION

The interplay of electron-electron interaction and the coupling of electrons to the lattice is a fascinating topic in condensed matter physics, with direct experimental relevance in compounds such as transition metal dichalcogenides.¹ Theoretically, this problem is particularly difficult in the case of non-Fermi liquids, e.g., Luttinger liquids realized in quasi-one-dimensional compounds. The difficulty is associated with the competition between the instantaneous Coulomb repulsion and the retarded, phonon-mediated attractive interaction.

The Holstein-Hubbard model is one of the most frequently studied models in this context. It combines a local electron-electron repulsion (with strength U), a nearest-neighbor hopping and a local density-displacement coupling between electrons and phonons. Even though it neglects anharmonicity effects and corrections due to incomplete screening,² it is believed to capture the key physics. In one dimension, where powerful numerical and analytical methods are available, existing work has mostly focused on the bipolaron problem of two electrons, see Refs. 3 and 4 for an overview, and the half-filled band.^{5–18} Some results for intermediate band fillings are also available.^{9,16,17,19,20} For vanishing Hubbard repulsion, the Holstein-Hubbard model reduces to Holstein's molecular crystal model²¹ which has been extensively studied at half filling, see Refs. 2,22–25 and references therein. The Holstein-Hubbard model may also be investigated in the framework of dynamical mean-field theory,^{26–31} although non-Fermi liquid physics and spatial correlations are not captured.

Interaction effects are dominant for a half-filled one-dimensional system.⁴¹ In the Hubbard model, a repulsive electron-electron interaction leads to a Mott insulator with dominant spin-density-wave correlations but no long-range order (a detailed definition of the various phases considered in the following is given in Sec. IV; see also Table I). If the interaction is attractive, arising from electron-phonon coupling in the limit of high phonon fre-

quencies, backscattering opens a spin gap, but the system remains metallic. Hirsch and Fradkin²² argue that the $U(1)$ charge symmetry is broken at finite phonon frequencies, so that long-range order can exist at $T = 0$ as a result of the Peierls instability.³² Alternatively, such a transition to a state with two electrons at every other site can result from a nearest-neighbor electron-electron repulsion that emerges from electron-phonon interaction. In the static limit of classical phonons, exactly solvable in mean-field theory, an insulating Peierls state exists for any nonzero electron-phonon coupling. To fully understand the role of quantum lattice fluctuations (a finite phonon frequency, as relevant for experiments) has turned out to be a complex problem that still poses a number of open questions.

Whereas early numerical results for the half-filled Holstein model suggested the existence of an insulating Peierls state for any nonzero coupling,²² in agreement with strong-coupling^{22,33} and renormalization group arguments,^{24,34} subsequent and more accurate treatments strongly suggest that lattice fluctuations destroy the charge-ordered state below a critical coupling strength.²³ Turning to the Holstein-Hubbard model, a metallic phase of the Holstein model should survive for small enough values of the electron repulsion, as predicted previously.^{5,35} Early numerical studies focused on large values of U where the system is only metallic at the single point of the Mott insulator to Peierls insulator transition.^{10,36} Evidence for a metallic phase, whose extent strongly depends on the phonon frequency, was reported later.^{8,11,17} Recently, work aiming at characterizing this intermediate phase has initiated a debate about the possibility of dominant superconducting correlations,^{15,17} the existence of a spin gap,¹² the validity of Luttinger liquid theory for retarded interactions,¹⁵ and the existence of a metallic phase.^{15,24,34}

The metallic phase is of particular interest in relation to superconductivity in quasi-one-dimensional or higher dimensional systems. Even though the continuous $U(1)$ gauge symmetry cannot be broken in one dimension,

dominant superconducting correlations imply a tendency toward superconductivity in higher-dimensional settings. Initial numerical results for the metallic phase in the Holstein-Hubbard model indicated a Luttinger liquid parameter $K_\rho > 1$,^{8,9,11,12} which suggests dominant pairing correlations. However, direct calculations of correlators instead reveal that charge-density-wave correlations dominate.^{15–17} This contradiction has been attributed to finite-size effects⁹ and logarithmic corrections¹⁵ due to the retarded nature of the phonon-mediated interaction. Dominant pair correlations together with $K_\rho > 1$ have been reported at quarter filling,³⁷ and degenerate pairing and charge correlations exist in the half-filled lattice Fröhlich model.²

Another controversial issue is the existence of a spin gap in the metallic phase, as a result of binding of electron pairs into singlet bipolarons. This would imply that the low-energy theory is that of a *Luther-Emery liquid* (a Luttinger liquid with gapped spin excitations but gapless charge excitations, see Table I),^{38,39} which has also been suggested as the appropriate description of the normal state of Peierls compounds (i.e., for $T > T_c$).⁴⁰ In the nonadiabatic limit, the mapping to the attractive Hubbard model implies a nonzero spin gap. For small interactions, the gap scales as⁴¹ $\Delta_\sigma \sim e^{-v_F/\mathcal{U}}$ where \mathcal{U} , the effective backscattering matrix element, can either be related to the attractive Hubbard interaction mediated by the phonons in the Holstein model, or to the net interaction resulting from the interplay of electron-phonon and electron-electron interaction in the Holstein-Hubbard model. In the static mean-field limit, a spin gap exists for any nonzero coupling. For finite and especially for low phonon frequencies, there are significant retardation effects. Similar to the destruction of the Peierls state by lattice fluctuations due to a reduction of umklapp scattering,^{23,41,42} the spin gap may be destroyed for small enough interactions by a renormalization of backscattering under the renormalization group flow. Another possible mechanism is the dissociation of bipolarons (a bound state always exists for exactly two electrons, but this bipolaron is spatially extended for weak coupling) due to mutual overlap, similar to polaron dissociation at finite band filling.^{43,44} On the other hand, in the low-energy limit, any finite phonon frequency may naively be argued to be irrelevant, leading back to the spin-gapped attractive Hubbard model.⁴⁵ There is also evidence from renormalization group calculations that retardation can enhance backscattering.²⁴

A gap that opens exponentially is of course very difficult to detect by numerical methods. Several previous works explicitly state that the metallic phase presumably has a finite spin gap.^{9,12,15} A crossover from gapless to gapped spin excitations inside the metallic region has also been proposed.^{11,46} Recently, a spin gap has been observed for all phonon frequencies in the quarter-filled Holstein model at intermediate electron-phonon coupling.³⁷

Here, the continuous-time quantum Monte Carlo (CTQMC) method is used to calculate the single-particle

spectral function as well as the dynamical charge and spin structure factors in all three phases of the Holstein-Hubbard model. Previous work focused on single-particle spectra^{10,13,14} and the optical conductivity.^{36,47} Additionally, arguments and numerical evidence for the existence of a spin gap in the entire metallic phase are presented. The paper is organized as follows: After briefly introducing the model and the method in Secs. II and III, the results are presented in Sec. IV, followed by the conclusions in Sec. V.

II. MODEL

In one dimension, the Holstein-Hubbard Hamiltonian can be written as

$$\hat{H} = -t \sum_{i\sigma} \left(c_{i\sigma}^\dagger c_{i+1\sigma} + \text{H.c.} \right) + U \sum_i \hat{n}_{i\uparrow} \hat{n}_{i\downarrow} \quad (1)$$

$$+ \sum_i \left(\frac{\hat{P}_i^2}{2M} + \frac{K \hat{Q}_i^2}{2} \right) - g \sum_i \hat{Q}_i (\hat{n}_i - 1).$$

The first and second terms constitute the Hubbard model, describing electrons with nearest-neighbor hopping t and local repulsion U . The third and fourth terms correspond to the lattice degrees of freedom and the electron-phonon coupling. The phonons are described as harmonic oscillators with frequency $\omega_0 = \sqrt{K/M}$, displacement \hat{Q}_i and momentum \hat{P}_i , and the coupling is of the density-displacement type proposed by Holstein;²¹ g is the coupling strength. The usual definitions $\hat{n}_{i\sigma} = c_{i\sigma}^\dagger c_{i\sigma}$, $\hat{n}_i = \sum_\sigma \hat{n}_{i\sigma}$, and $n = \langle \hat{n}_i \rangle$ are used.

Using the path-integral representation, an effective, frequency-dependent electron-electron interaction

$$U(\omega) = U + \lambda W \frac{\omega_0^2}{\omega^2 - \omega_0^2} \quad (2)$$

can be derived, where $\lambda = g^2/(KW)$ is a dimensionless electron-phonon coupling constant and $W = 4t$ is the free bandwidth. In the nonadiabatic limit (high phonon frequency, $\omega_0 \rightarrow \infty$) or at low energies ($\omega \rightarrow 0$), this interaction reduces to an instantaneous attractive or repulsive Hubbard interaction $U_\infty = U - \lambda W$. In the following, the hopping t is taken as the unit of energy, and the lattice constant and \hbar are set equal to one.

III. METHOD

The model (1) can be studied with the CTQMC method in the interaction-expansion formulation.⁴⁸ This method is free of Trotter errors, and has been successfully applied to electron-phonon lattice models.^{2,37,46,49} The bosonic degrees of freedom are integrated out exactly (without a cutoff for the bosonic Hilbert space), and the resulting fermionic model with retarded electron-electron interactions is simulated.⁵⁰ Methodological details can be

found in previous publications^{2,37,46,49,50} and a review.⁵¹ The numerical effort scales with the average expansion order, making large system sizes accessible at weak coupling. The method gives exact results with statistical errors for imaginary-time correlation functions.

The results below have been obtained at low but finite temperatures $20 < \beta t < 162$; the inverse temperature is specified in each figure caption. When comparing different system sizes, the ratio $\beta t/L$ has been kept constant. The system size was $L = 30$ or $L = 50$ for excitation spectra, and $L = 30$ – 162 for static correlation functions. Each QMC run was started with a zero-vertex configuration, and equilibration was carried out until the acceptance rates for addition and removal of a single vertex have become equal to within one percent. Measurements were collected from independent, parallel runs (typically 31) for each set of parameters. For the most demanding parameters considered (Fig. 7), about 500 bins of 150 sweeps each were recorded (with measurements taken at the end of each sweep). A sweep corresponded to 1000 proposed Monte Carlo updates (addition or removal of a single vertex, or 32 attempted flips of auxiliary Ising spins⁵⁰). Error analysis included the usual binning and jackknife procedures to avoid underestimation of statistical errors due to autocorrelations. Error bars shown indicate the standard error.

Spectral functions were obtained by applying a stochastic maximum-entropy method⁵² to the imaginary-time Green function data and their covariance matrix. Convergence of statistical errors was achieved over at least three orders of magnitude. A flat default model was used, and the renormalization parameter was chosen to (approximately) achieve $\chi^2 = L_\tau$, where L_τ is the number of points on the imaginary time axis.

The static correlation functions of interest are

$$S_\rho(r) = \langle (\hat{n}_r - n)(\hat{n}_0 - n) \rangle, \quad (3)$$

$$S_\sigma^{zz}(r) = \langle \hat{S}_r^z \hat{S}_0^z \rangle,$$

$$S_\sigma^{xx}(r) = \langle \hat{S}_r^x \hat{S}_0^x \rangle,$$

$$P(r) = \langle \hat{\Delta}_r^\dagger \hat{\Delta}_0 \rangle \quad (\hat{\Delta}_r = c_{r\uparrow}^\dagger c_{r\downarrow}^\dagger),$$

measuring charge, spin, and s-wave pairing correlations, as well as their Fourier transforms. In combination with the maximum entropy method,⁵² excitation spectra can be calculated, including the dynamical charge structure factor ($\Delta_{ji} = E_j - E_i$),

$$S_\rho(q, \omega) = \frac{1}{Z} \sum_{ij} |\langle i | \hat{\rho}_q | j \rangle|^2 e^{-\beta E_j} \delta(\Delta_{ji} - \omega), \quad (4)$$

$$\hat{\rho}_q = \frac{1}{\sqrt{L}} \sum_r e^{iqr} (\hat{n}_r - n), \quad (5)$$

the dynamical spin structure factor,

$$S_\sigma(q, \omega) = \frac{1}{Z} \sum_{ij} |\langle i | \hat{S}_q^z | j \rangle|^2 e^{-\beta E_j} \delta(\Delta_{ji} - \omega), \quad (6)$$

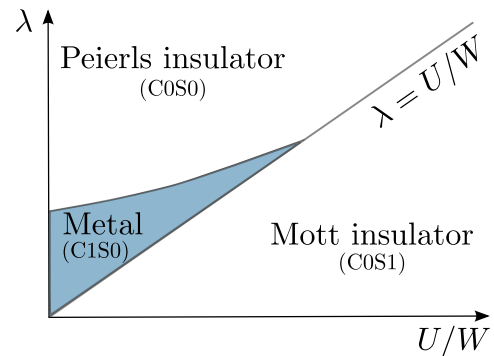


FIG. 1: (Color online) Schematic ground-state phase diagram of the half-filled, one-dimensional Holstein-Hubbard model with a finite phonon frequency, as suggested by numerical simulations.^{8,9,11,12,17} For $U/W \gtrsim \lambda$, the system is a Mott insulator with dominant, power-law SDW correlations and a nonzero charge gap Δ_ρ (the notation C0S1 is explained in the text and in Table I). For $\lambda \gg U/W$, the ground state is a Peierls insulator with long-range $2k_F$ charge correlations and nonzero charge and spin gaps Δ_ρ , Δ_σ . For small U/W and λ (the scale depends on the phonon frequency), a metallic phase with gapless charge excitations exists for $\lambda \geq U/W$ ($U_\infty < 0$). Here it is argued that the entire metallic phase has a spin gap.

and the single-particle spectral function

$$A(k, \omega) = \frac{1}{Z} \sum_{ij\sigma} |\langle i | c_{k\sigma} | j \rangle|^2 (e^{-\beta E_i} + e^{-\beta E_j}) \delta(\Delta_{ji} - \omega). \quad (7)$$

Here $|i\rangle$ denotes an eigenstate with energy E_i .

IV. RESULTS

Figure 1 shows a schematic phase diagram of the half-filled Holstein-Hubbard model. Exact numerical investigations^{8,9,11,17} suggest the existence of three different phases at finite phonon frequencies. These phases can be characterized and distinguished by the presence or absence of an excitation gap for single-particle (Δ_{sp}), charge (Δ_ρ) and/or spin excitations (Δ_σ) with zero momentum, see Table I. Following Balents and Fisher,⁵³ the notation $CxSy$ is used, where x (y) is the number of gapless charge (spin) modes (with $x, y = 0, 1$ for a strictly one-dimensional system). Since a two-particle gap for either spin or charge excitations also implies a nonzero single-particle gap Δ_{sp} , knowledge of Δ_ρ and Δ_σ is sufficient. Finally, because low-energy charge transport is determined by long-wavelength density fluctuations, the charge gap Δ_ρ further distinguishes metallic ($\Delta_\rho = 0$) and insulating ($\Delta_\rho > 0$) states.

The *Mott insulator* in Fig. 1 exists for repulsive interactions ($U_\infty \gtrsim 0$). It falls into the category C0S1, with a nonzero charge gap Δ_ρ (and hence $\Delta_{\text{sp}} > 0$) reflecting the energy cost for doubly occupied sites, a vanishing spin

TABLE I: The different phases discussed in the text can be distinguished by the absence or presence of gaps for charge, spin, and single-particle excitations. The latter are denoted as Δ_ρ , Δ_σ , and Δ_{sp} , respectively. The last column gives the corresponding class in the Balents-Fisher notation.⁵³

Phase	Δ_ρ	Δ_σ	Δ_{sp}	Class
Luttinger liquid	zero	zero	zero	C1S1
Luther-Emery liquid	zero	nonzero	nonzero	C1S0
Mott insulator	nonzero	zero	nonzero	C0S1
Peierls insulator	nonzero	nonzero	nonzero	C0S0

gap $\Delta_\sigma = 0$, and dominant, power-law spin-density-wave (SDW) correlations.

The intermediate *metallic phase* exists for small enough λ and U , with the explicit scale depending on ω_0/t .^{8,9,11,17} In one dimension, a metallic phase can either correspond to a *Luttinger liquid* with $\Delta_{\text{sp}} = \Delta_\rho = \Delta_\sigma = 0$ (C1S1), or to a *Luther-Emery liquid* with $\Delta_\rho = 0$ but $\Delta_{\text{sp}}, \Delta_\sigma > 0$ (C1S0).⁴¹ The Luther-Emery liquid can be understood as a liquid of bosons, each consisting of two electrons bound into a spin singlet. The excitation spectrum for these bosons (corresponding to bipolarons in electron-phonon models) is gapless within the metallic phase (hence $\Delta_\rho = 0$), but the binding of electrons into pairs gives rise to gaps for (electronic) single-particle and spin excitations ($\Delta_{\text{sp}}, \Delta_\sigma > 0$). The results presented below suggest that in the Holstein and Holstein-Hubbard models, the metallic phase is a Luther-Emery liquid (C1S0), except for the line $U_\infty = 0$, which belongs to the Luttinger liquid class C1S1.

The extent of the metallic phase increases with increasing phonon frequency.^{8,9,11,17} This can be ascribed to the suppression of charge order (the latter is generally favored for $U_\infty < 0$) due to enhanced lattice fluctuations. These fluctuations have been shown²³ to destroy the Peierls state of the half-filled Holstein model below a critical value of λ . The numerical results suggest that the metallic region exists in the Holstein-Hubbard model for $U_\infty < 0$, and is adiabatically connected to that of the Holstein model ($U = 0$). For $\omega_0/t = 5$, the density-matrix renormalization group (DMRG)¹¹ yields a larger metallic region than the QMC simulations,⁹ whereas for $\omega_0/t = 0.5$ the two methods are in quite good agreement. These two frequencies will also be considered here. Finally, at the tricritical point where the Mott, Peierls and metallic phases intersect, a first-order phase transition has been reported.⁹

When the electron-phonon interaction dominates ($U_\infty \ll 0$), the system is a *Peierls insulator* with nonzero single-particle, charge and spin gaps (C0S0). The origin of the spin gap is again a pairing of electrons into spin singlets, similar to the Luther-Emery phase. At $T = 0$, the Peierls state has long-range charge-density-wave (CDW) order with period $q = 2k_F$, corresponding to a pair of electrons residing at every other lattice site. As in the mean-field Peierls problem,^{22,32} excitations out of the en-

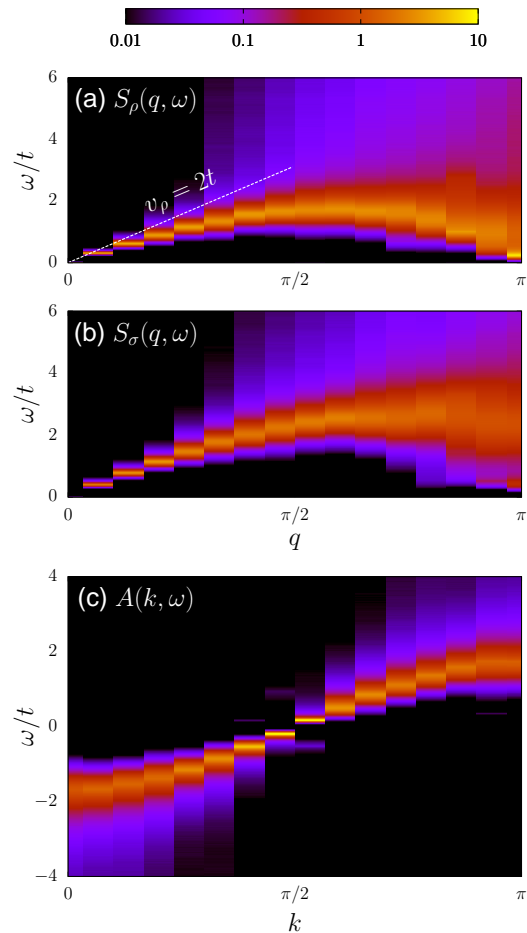


FIG. 2: (Color online) (a) Dynamical charge structure factor, (b) dynamical spin structure factor, and (c) single-particle spectral function for $\omega_0/t = 5$, $U/t = 1$, and $\lambda = 0.5$, corresponding to the *metallic phase* (C1S0).^{9,11} Here $L = 30$, $\beta t = 30$. The dashed line indicates the charge velocity in the noninteracting case ($\lambda = 0$, $U = 0$).

ergetically favored $2k_F$ state cost a finite energy Δ_ρ .

A. Spectra in the metallic phase

Figure 2 shows the dynamical charge and spin structure factors, defined in Eqs. (4) and (6), as well as the single-particle spectral function [Eq. (7)] in the nonadiabatic regime $\omega_0/t = 5$ and for $U/t = 1$, $\lambda = 0.5$. For these parameters, the metallic phase has been found to extend up to $\lambda \approx 0.65$ by QMC simulations,⁹ and up to $\lambda \approx 0.9$ by DMRG calculations.¹¹

The dynamical charge structure factor, plotted in Fig. 2(a), reveals a gapless mode at long wavelengths. Its velocity, v_ρ , is noticeably smaller than the noninteracting value $v_\rho = 2t$ as a result of the enhanced mass of bipolarons. At $q = \pi = 2k_F$, there is an almost completely softened excitation with dominant spectral weight, which indicates strong but power-law charge correlations with

period $2k_F$ that are a precursor of the ordered Peierls phase. The dynamical spin structure factor in Fig. 2(b) also shows a linear mode. A possible spin gap is too small to be visible for these parameters.

Figure 3 shows the excitation spectra for a stronger electron-phonon coupling $\lambda = 0.875$, closer to (potentially on) the DMRG phase boundary for the metallic phase.¹¹ The charge structure factor still appears gapless, signaling metallic behavior, with an even smaller charge velocity and stronger softening at $q = 2k_F$ than in Fig. 2(a). The spin structure factor has developed a well visible gap at long wavelengths, which is also reflected in the corresponding single-particle spectrum in Fig. 3(c). The existence of bound singlets, as reflected by the spin gap, makes bipolarons the low-energy degrees of freedom. The corresponding Drude weight strongly depends on the phonon frequency.³⁷ An important point concerning Figs. 2 and 3 is that a gapless mode with significant Drude weight exists in $S_\rho(q, \omega)$ near $q = 0$. In contrast, the spectrum in the insulating Peierls phase [see Fig. 7(a)] exhibits a strong depletion of spectral weight and a finite gap for long-wavelength charge excitations.

The metallic region shrinks with decreasing phonon frequency.^{9,11,17} To study the adiabatic regime, a value $\omega_0/t = 0.5$ is considered, for which the extent of the metallic phase is known.^{9,11} For $U/t = 0.2$, it exists up to $\lambda \approx 0.25$.¹¹ Since the spin gap increases on approaching the Peierls phase (see discussion above for $\omega_0/t = 5$), an electron-phonon coupling close to the phase boundary ($\lambda = 0.225$) is chosen.

The charge velocity v_ρ in Fig. 4(a) is almost unchanged compared to the noninteracting case, which can be understood in terms of the rather small bare coupling constant g . Hence, the electrons are only loosely bound into large bipolarons. An important difference to the case $\omega_0/t = 5$ considered before is that the charge structure factor in Fig. 4(a) reveals the renormalized phonon frequency at low energies. The latter is partially softened at $q = 2k_F$, which is a previously noted precursor effect of the Peierls transition.^{49,54–56}

The spin structure factor in Fig. 4(b) appears to be gapless (although it will be argued below that a finite spin gap exists throughout the metallic phase), with a weakly renormalized, linear low-energy mode. Finally, the single-particle spectrum in Fig. 4(c) also appears gapless, with small but visible signatures of the hybridized polaron modes located near $\omega = \pm\omega_0$.⁴⁶

Previous numerical calculations of excitation spectra of the half-filled, metallic Holstein-Hubbard model were restricted to the single-particle spectrum,¹³ and showed in particular that spin-charge separation is only visible for large values of λ (this in turn requires a large ratio ω_0/t for a metallic state to exist), in accordance with simulations at quarter filling.⁴⁶ This conclusion explains the absence of such features in the present results. The spectrum was also calculated at $U = 0.2$. Analytical results include the exact spectrum of a Luttinger liquid (i.e., without a spin gap) coupled to phonons,⁵⁷ as well as ap-

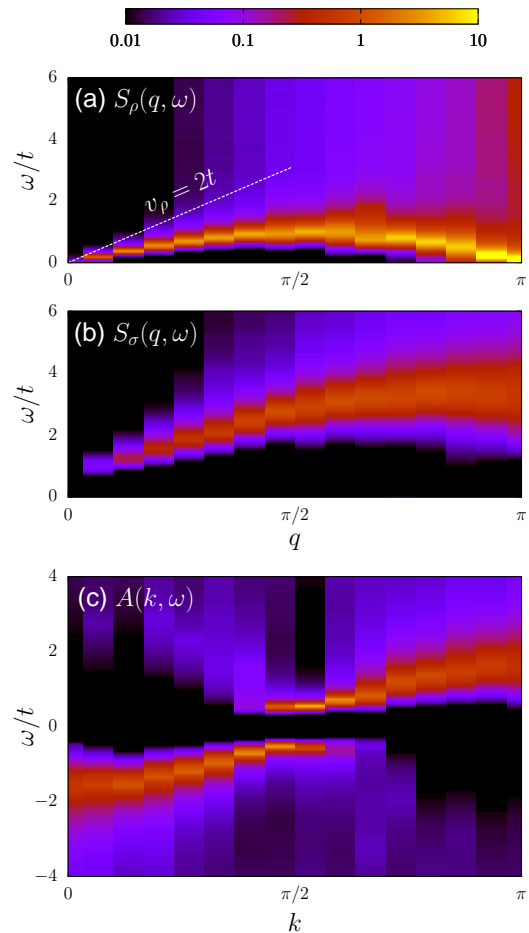


FIG. 3: (Color online) (a) Dynamical charge structure factor, (b) dynamical spin structure factor, and (c) single-particle spectral function for $\omega_0/t = 5$, $U/t = 1$, and $\lambda = 0.875$, corresponding to the *metallic phase* (C1S0).¹¹ Here $L = 30$, $\beta t = 20$. The dashed line indicates the charge velocity in the noninteracting case ($\lambda = 0$, $U = 0$).

proximate results for the spectral function of the Luther-Emery liquid.⁴⁰ The latter work predicts that branch cuts may be regularized by the existence of a gap. Interestingly, for small λ where the spin gap is not resolved and where spin-charge separation is not detected in numerical simulations, the spectrum is very well described by analytical results for a spinless Luttinger liquid coupled to phonons,⁵⁷ and closely resembles the spectrum of the spinless Holstein model.⁴⁹

B. Spin gap in the metallic phase

A spin gap is visible in the dynamical correlation functions shown above, at least close to the Peierls phase boundary. The initially exponential dependence of this gap on the interaction strength and restrictions in system size make it difficult to detect the spin gap at weak coupling by considering excitation spectra. Instead, evidence

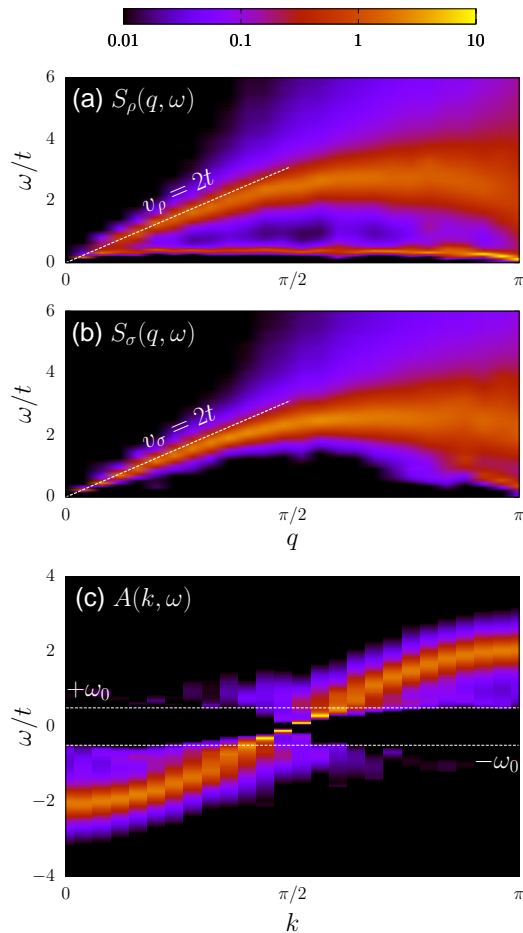


FIG. 4: (Color online) (a) Dynamical charge structure factor, (b) dynamical spin structure factor, and (c) single-particle spectral function for $\omega_0/t = 0.5$, $U/t = 0.2$, and $\lambda = 0.225$, corresponding to the *metallic phase* (C1S0). Here $L = 50$, $\beta t = 50$. The dashed lines in (a) and (b) indicate the charge and spin velocities in the noninteracting case ($\lambda = 0$, $U = 0$), respectively. The horizontal lines in (c) mark $\pm\omega_0$.

for a nonzero spin gap in the metallic Holstein-Hubbard model comes from numerical results for the Luttinger liquid parameter K_σ , which can in principle be determined from the spin structure factor and finite-size extrapolation as $K_\sigma = \lim_{L \rightarrow \infty} \pi S_\sigma(q_1)/q_1$, with $q_1 = 2\pi/L$. For the half-filled Hubbard model, were complications such as retarded electron-electron interactions are absent, numerical simulations generically give $\pi S_\sigma(q_1)/q_1 > 1$ for $U > 0$, $\pi S_\sigma(q_1)/q_1 < 1$ for $U < 0$, and $\pi S_\sigma(q_1)/q_1 = 1$ exactly at $U = 0$.⁹ In particular, although logarithmic corrections make it hard to demonstrate $K_\sigma = 1$ or 0 in the spin gapless and spin gapped phases, respectively, the finite-size estimates always decrease with increasing system size. Therefore, for the repulsive case $U > 0$, $\pi S_\sigma(q_1)/q_1$ slowly approaches the value 1 implied by spin rotation symmetry from above, whereas for the attractive case $U < 0$, $\pi S_\sigma(q_1)/q_1$ deviates more and more from 1. Within a low-energy theory, and given spin

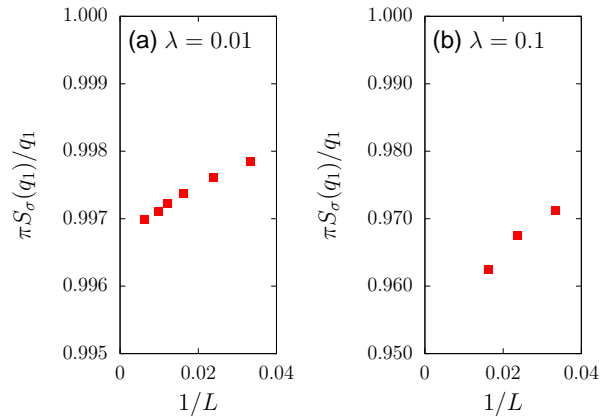


FIG. 5: (Color online) Renormalized spin structure factor $\pi S_\sigma(q_1)/q_1$ at $q_1 = 2\pi/L$, related to K_σ via $K_\sigma = \lim_{L \rightarrow \infty} \pi S_\sigma(q_1)/q_1$, as a function of inverse system size in the metallic phase of the Holstein model. Results are for $\beta t = L$, $\omega_0/t = 0.5$, $U = 0$, and (a) $\lambda = 0.01$, (b) $\lambda = 0.1$.

symmetry, the latter result can only be understood in terms of $K_\sigma = 0$ and a spin gap. Similar behavior can also be observed beyond the Hubbard model, and values $\pi S_\sigma(q_1)/q_1 < 1$ have been argued to represent empirical evidence for a spin gap.⁵⁸ For a more detailed discussion see Refs. 9,58.

Figure 5 shows the system size dependence of $\pi S_\sigma(q_1)/q_1$ in the adiabatic regime ($\omega_0/t = 0.5$) of the Holstein model in the metallic phase. Even for very weak coupling $\lambda = 0.01$, $\pi S_\sigma(q_1)/q_1 < 1$ and monotonically decreasing with increasing system size. At stronger coupling $\lambda = 0.1$, the size dependence is significantly more pronounced. A similar picture persists for larger phonon frequencies. The spin gap has also been measured directly by means of the DMRG method. While Δ_σ is clearly finite for selected parameters in the metallic region, it is difficult to decide if this is true of the whole metallic phase.^{11,12} In particular, the exponential dependence of the gap on the coupling makes it practically impossible to detect the critical point directly from Δ_σ .

To provide further evidence for the existence of a spin gap, it is useful to consider the real-space correlation functions. In a gapless Luttinger liquid, the slowest decaying correlations are given by⁴⁵

$$\begin{aligned}
 R_{\text{CDW}}(r) &\sim \cos(2k_{\text{F}}r)r^{-K_\rho - K_\sigma}, \\
 R_{\text{SDW}}^{\text{zz}}(r) &\sim \cos(2k_{\text{F}}r)r^{-K_\rho - K_\sigma}, \\
 R_{\text{SDW}}^{\text{xy}}(r) &\sim \cos(2k_{\text{F}}r)r^{-K_\rho - 1/K_\sigma}, \\
 R_{\text{SS}}(r) &\sim r^{-1/K_\rho - K_\sigma}.
 \end{aligned} \tag{8}$$

For a generic spin-rotation invariant system with $K_\sigma = 1$, spin and charge correlations are degenerate, and dominate over pairing correlations if $K_\rho < 1$. On the other hand, attractive interactions ($K_\rho < 1$) lead to dominant pairing correlations. Additional complications are logarithmic corrections arising from marginally relevant

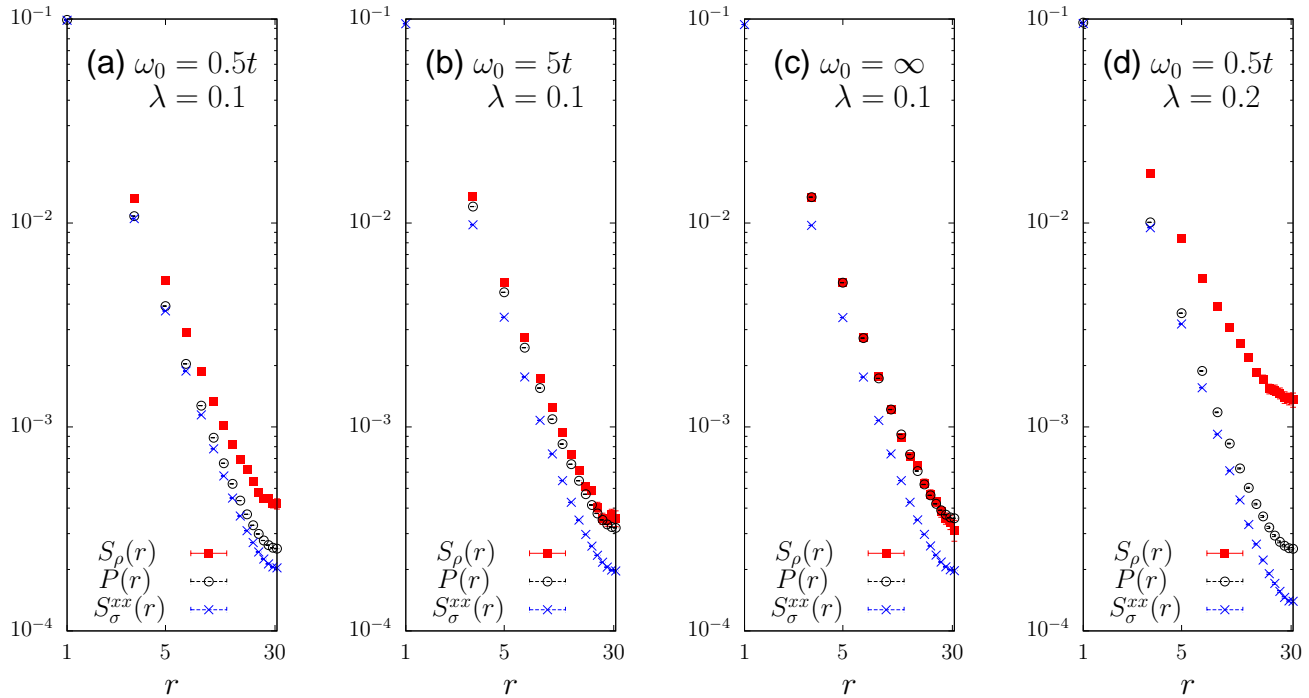


FIG. 6: (Color online) Real-space charge, pairing, and spin correlations (all rescaled by a factor $1/2$) for (a) $U = 0$, $\lambda = 0.1$, $\omega_0 = 0.5t$, (b) $U = 0$, $\lambda = 0.1$, $\omega_0 = 5t$, both corresponding to the metallic phase of the Holstein model. (c) The same correlation functions for the attractive Hubbard model with $U = -0.4t$. (d) As in (a), but for $U = 0$, $\omega_0 = 0.5t$, and $\lambda = 0.2$. Results are for $\beta t = L = 62$. Spin correlations in the z and x directions are identical within error bars; S_{σ}^{xx} is shown because of its smaller error bars.

operators. In the repulsive Hubbard model, such corrections cause spin correlations to dominate over charge correlations.⁵⁹ As pointed out by Voit,⁴⁰ dominant $q = 2k_F$ CDW correlations cannot occur in a gapless Luttinger liquid. (Although logarithmic corrections could in principle favor charge over spin correlations, there is no known example of such behavior. Moreover, such corrections would not explain $K_{\sigma} < 1$.)

In contrast, due to the exponential suppression of spin correlations, a Luttinger liquid with a gap for spin excitations supports dominant $2k_F$ charge correlations. In terms of the low-energy model, this case arises when attractive backscattering is taken into account.³⁸ The corresponding model is often referred to as a Luther-Emery model. A familiar example is the attractive Hubbard model. That attractive backscattering can originate from electron-phonon interaction is illustrated by the previously mentioned explicit relation between the Holstein model and the attractive Hubbard model. To obtain the correlation functions of the a Luther-Emery liquid, the spin gap can formally be accounted for by setting $K_{\sigma} = 0$, leading to⁴⁵ $R_{\text{CDW}}(r) \sim \cos(2k_F r)r^{-K_{\rho}}$ and $R_{\text{SS}}(r) \sim r^{-1/K_{\rho}}$, see also Eq. (8). Hence, neglecting possible logarithmic corrections, repulsive (attractive) interactions lead to dominant charge (pairing) correlations.

Results for the charge, spin and pairing correlation functions are shown in Fig. 6. Figures 6(a) and (b) cor-

respond to the adiabatic ($\omega_0/t = 0.5$) and the nonadiabatic regime ($\omega_0/t = 5$), respectively. To be able to explore very weak interactions U_{∞} , it is advantageous to consider $U = 0$, so that the metallic phase exists down to $\lambda = 0$. This choice also eliminates any uncertainties about the phase boundaries of the metallic region. For the coupling $\lambda = 0.1$ chosen, charge correlations dominate over pairing and spin correlations, as expected for a Luther-Emery liquid with repulsive interactions. This dominance is more pronounced for $\omega_0/t = 0.5$ [Fig. 6(a)] than for $\omega_0/t = 5$ [Fig. 6(b)] because the system is closer to the Peierls phase, and cannot be explained by a rescaling of the constant (i.e., independent of r) prefactors of $2k_F$ correlations in the charge and spin channels. The results are qualitatively similar also at weaker interactions (the values investigated where as small as $\lambda = 0.01$), but it becomes increasingly more difficult to distinguish the different correlation functions on finite systems.

For comparison, Fig. 6(c) presents the same correlation functions for the attractive Hubbard model with $U = -\lambda W = -0.4t$, corresponding to the limit $\omega_0 = \infty$ at the same coupling $\lambda = 0.1$ used in Figs. 6(a), (b). Whereas spin correlations are again clearly suppressed, the mapping between the attractive and the repulsive Hubbard model at half filling implies a degeneracy of charge and pairing correlations that is captured, within statistical errors, by the numerical data. Finally,

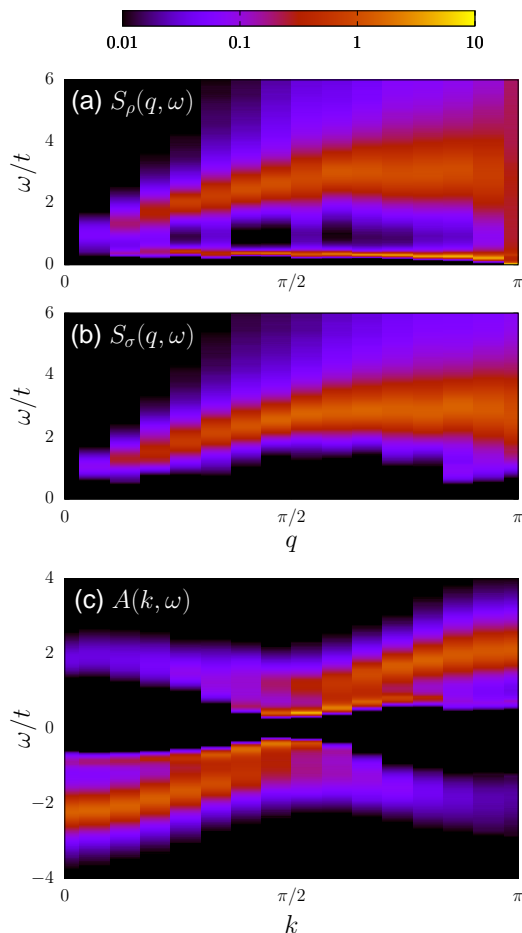


FIG. 7: (Color online) (a) Dynamical charge structure factor, (b) dynamical spin structure factor, and (c) single-particle spectral function for $\omega_0/t = 0.5$, $U/t = 0.2$, and $\lambda = 0.4$, corresponding to the *Peierls insulator* (C0S0). Here $L = 30$, $\beta t = 30$.

Fig. 6(d) shows results at a stronger coupling $\lambda = 0.2$, for which charge correlations and the suppression of spin correlations are much more pronounced. The exponential decay of spin correlations has been observed before in DMRG calculations.¹⁷

The results for $\pi S_\sigma(q_1)/q_1$ and the real-space correlation functions are fully compatible with the existence of a spin gap throughout the metallic phase. In particular, the behavior of these observables is essentially identical to the attractive Hubbard model, for which the existence of a spin gap is well established. In contrast to the gapless Luttinger liquid model, the Luther-Emery model hence provides a consistent description of the numerical data. The existence of a spin gap for any nonzero electron-phonon coupling in the Holstein model has also been predicted based on renormalization group calculations.^{24,60}

The above results suggest that the half-filled, metallic Holstein model behaves as a repulsive Luther-Emery liquid, with dominant charge correlations, and a nonzero spin gap in the thermodynamic limit that suppresses spin

correlations with respect to charge and pairing correlations. Assuming that the metallic phase is the same at $U = 0$ and $U > 0$ leads to the conclusion that the whole metallic region of the Holstein-Hubbard model is a Luther-Emery liquid. The exponential length scale related to the spin gap is expected to lead to a crossover (as a function of system size) from the correlation functions (8), as appropriate for a system with gapless spin excitations, to the corresponding analytical results for the Luther-Emery liquid.⁴⁵ In particular, the relation $\alpha_{\text{CDW}}\alpha_{\text{SS}} = 1$, expected for a Luther-Emery liquid, is not obeyed by the numerically determined power-law exponents. Whereas this fact has previously been attributed to retardation effects,¹⁵ it can be expected to be a general problem associated with finite-size simulations of Luther-Emery liquids.

C. Spectra in the Peierls phase

The single-particle spectral function in the Peierls phase has been calculated before using numerical methods.^{2,10} Bosonization results for the spectrum of a quarter-filled CDW insulator are also available.⁶¹ The dynamical charge structure factor has been studied for the spinless Holstein model.⁴⁹ Using the CTQMC method, the Peierls state is most accessible in the adiabatic regime. Specifically, $\omega_0/t = 0.5$, $\lambda = 0.4$, and $U/t = 0.2$ are considered, and results are shown in Fig. 7.

The dynamical charge structure factor in Fig. 7(a) is characterized by a finite gap and strongly suppressed spectral weight for long-wavelength charge excitations, and by a soft phonon mode with gapless excitations at $q = 2k_F$. Similar to the metallic Luther-Emery phase, the Peierls state has a finite (but larger) spin gap, see Fig. 7(b). Compared to the spin structure factor in the metallic phase, Fig. 4(b), there is also a finite gap for spin excitations with $q = 2k_F$.

The single-particle spectrum in Fig. 7(c) reveals the expected Peierls gap, as well as clear signatures of backfolded shadow bands at high energies—as a result of dimerization⁶²—and soliton excitations at low energies. The latter have previously been observed in the spinless Holstein model,⁴⁹ and the extended Holstein model with nonlocal interactions,² and distinguish the otherwise qualitatively (apart from the size of the single-particle gap) similar spectra of the metallic phase [Fig. 4(c)] and the Peierls phase [Fig. 7(c)].

D. Spectra in the Mott phase

The excitation spectra in the Mott phase are shown in Fig. 8, for the parameters $\omega_0/t = 5$, $\lambda = 0.25$, and $U/t = 4$. The single-particle spectrum in this phase has previously been calculated.^{10,13,14}

In accordance with the discussion of the phase diagram at the beginning of Sec. IV, the results in Fig. 8

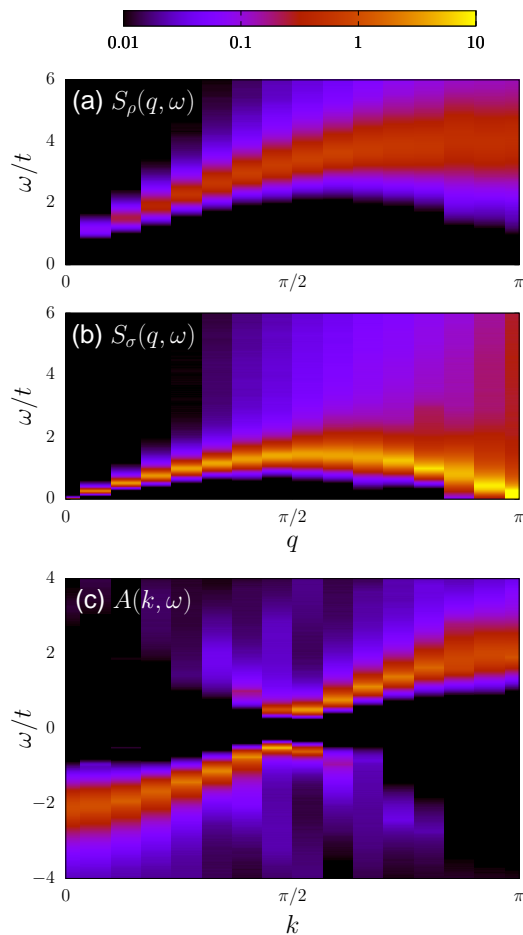


FIG. 8: (Color online) (a) Dynamical charge structure factor, (b) dynamical spin structure factor, and (c) single-particle spectral function for $\omega_0/t = 5$, $U/t = 4$, and $\lambda = 0.25$, corresponding to the *Mott insulator* (C0S1). Here $L = 30$, $\beta t = 20$.

reveal gapped charge excitations but gapless spin excitations, i.e., just opposite to the metallic phase shown in Fig. 3. Although the spin symmetry is not broken in the Mott phase, the spin structure factor reveals gapless spin excitations at $q = 2k_F$ reminiscent of the soft phonon mode related to long-range charge order in Fig. 7(a). For the value $\omega_0/t = 5$ considered, the renormalized phonon mode is not visible in $S_\rho(q, \omega)$, and it is strongly suppressed compared to the Peierls state even for $\omega_0/t = 0.5$ (data not shown).

The single-particle spectrum in Fig. 8(c) bears a close resemblance to the results for the Hubbard model with the same $U/t = 4$,⁶³ although signatures of spin-charge separation are suppressed here as a result of a reduced, effective interaction ($U_\infty/t = 3$) and thermal fluctuations at $T > 0$. The effects of the latter are quite subtle for intermediate values of U/t .⁶³ Instead of the pronounced backfolded shadow bands related to long-range charge order in the Peierls state, Fig. 7(c), there is rather incoherent spectral weight with no clear dispersion. Addition-

ally, the hallmark soliton excitations visible in Fig. 7(c) are completely absent.

V. CONCLUSIONS

The single- and two-particle excitation spectra of the one-dimensional, half-filled Holstein-Hubbard model have been calculated with the continuous-time quantum Monte Carlo method. The spectra in the metallic phase are consistent with a Luther-Emery liquid that has gapless charge excitations but gapped spin excitations with a gap that opens exponentially as a function of the interaction strength. In the Peierls phase, the spectra reveal both a charge and a spin gap, and a soft charge mode at $q = 2k_F$. The single-particle spectral function reveals backfolded shadow bands and soliton excitations. The Mott phase has a charge gap but no spin gap, as well as a soft spin mode despite the absence of long-range order. No clear signatures of spin-charge separation were observed.

The static charge and spin correlation functions have been calculated on rather large systems and reveal dominant $2k_F$ charge correlations even for very weak coupling. Because such behavior cannot occur in a generic Luttinger liquid, this observation can be regarded as evidence for a nonzero spin gap.⁴⁵ In particular, the behavior of these correlation functions is essentially the same as for the attractive Hubbard model (for which the existence of a spin gap is generally accepted) even for low phonon frequencies. When combined with the fact that the Luttinger parameter K_σ is found to be less than unity even for very weak coupling, the numerical data are naturally explained by assuming that the metallic phase of the Holstein-Hubbard model is a Luther-Emery liquid, with electrons paired into singlet bipolarons. Earlier reports of both gapless and gapped metallic regions^{11,46} can be attributed to the exponentially small size of the gap which makes its detection very demanding. The existence of a nonzero spin gap also has important implications for the low-energy description of this model. In particular, the spin gap is not captured by the exact results available for the spectral function of the Luttinger model with phonons.⁵⁷ Finally, given the relevance of backscattering at any band filling, the Luther-Emery description can be expected to be generic for metallic phases in Holstein-type models, in accordance with the suggestive physical picture of electron pairs that are bound into bipolarons.

Acknowledgments

Computer time at the Jülich Supercomputing Centre and financial support from the DFG (Grant No. Ho 4489/2-1) are gratefully acknowledged, as are discussions with S. Ejima, H. Fehske, V. Meden, A. Sandvik, D. Schuricht, S. Wessel, and, in particular, F. Essler.

- ¹ B. Sipoš, A. F. Kusmartseva, A. Akrap, H. Berger, L. Forro, and E. Tutis, *Nature Mat.* **7**, 960 (2008).
- ² M. Hohenadler, F. F. Assaad, and H. Fehske, *Phys. Rev. Lett.* **109**, 116407 (2012).
- ³ M. Hohenadler and W. von der Linden, *Phys. Rev. B* **71**, 184309 (2005).
- ⁴ J. T. Devreese and A. S. Alexandrov, *Rep. Prog. Phys.* **72**, 066501 (2009).
- ⁵ F. Guinea, *J. Phys. C: Solid State Phys.* **16**, 4405 (1983).
- ⁶ J. E. Hirsch, *Phys. Rev. B* **31**, 6022 (1985).
- ⁷ J. Stein, *Europhys. Lett.* **39**, 413 (1997).
- ⁸ R. T. Clay and R. P. Hardikar, *Phys. Rev. Lett.* **95**, 096401 (2005).
- ⁹ R. P. Hardikar and R. T. Clay, *Phys. Rev. B* **75**, 245103 (2007).
- ¹⁰ H. Fehske, G. Wellein, G. Hager, A. Weiße, and A. R. Bishop, *Phys. Rev. B* **69**, 165115 (2004).
- ¹¹ H. Fehske, G. Hager, and E. Jeckelmann, *Europhys. Lett.* **84**, 57001 (2008).
- ¹² S. Ejima and H. Fehske, *J. Phys. Conf. Ser.* **200**, 012031 (2010).
- ¹³ W. Q. Ning, H. Zhao, C. Q. Wu, and H. Q. Lin, *Phys. Rev. Lett.* **96**, 156402 (2006).
- ¹⁴ H. Matsueda, T. Tohyama, and S. Maekawa, *Phys. Rev. B* **74**, 241103 (2006).
- ¹⁵ K.-M. Tam, S.-W. Tsai, and D. K. Campbell, *Phys. Rev. B* **84**, 165123 (2011).
- ¹⁶ M. Tezuka, R. Arita, and H. Aoki, *Phys. Rev. Lett.* **95**, 226401 (2005).
- ¹⁷ M. Tezuka, R. Arita, and H. Aoki, *Phys. Rev. B* **76**, 155114 (2007).
- ¹⁸ A. Payeur and D. Sénéchal, *Phys. Rev. B* **83**, 033104 (2011).
- ¹⁹ S. Reja, S. Yarlagadda, and P. B. Littlewood, *Phys. Rev. B* **84**, 085127 (2011).
- ²⁰ S. Reja, S. Yarlagadda, and P. B. Littlewood, *Phys. Rev. B* **95**, 096401 (2012).
- ²¹ T. Holstein, *Ann. Phys. (N.Y.)* **8**, 325; **8**, 343 (1959).
- ²² J. E. Hirsch and E. Fradkin, *Phys. Rev. B* **27**, 4302 (1983).
- ²³ E. Jeckelmann, C. Zhang, and S. R. White, *Phys. Rev. B* **60**, 7950 (1999).
- ²⁴ I. P. Bindloss, *Phys. Rev. B* **71**, 205113 (2005).
- ²⁵ K.-M. Tam, S.-W. Tsai, D. K. Campbell, and A. H. Castro Neto, *Phys. Rev. B* **75**, 161103 (2007).
- ²⁶ D. Meyer, A. C. Hewson, and R. Bulla, *Phys. Rev. Lett.* **89**, 196401 (2002).
- ²⁷ W. Koller, D. Meyer, Y. Ono, and A. Hewson, *Euro. Phys. Lett.* **66**, 559 (2004).
- ²⁸ W. Koller, D. Meyer, and A. C. Hewson, *Phys. Rev. B* **70**, 155103 (2004).
- ²⁹ M. Capone, G. Sangiovanni, C. Castellani, C. Di Castro, and M. Grilli, *Phys. Rev. Lett.* **92**, 106401 (2004).
- ³⁰ P. Werner and A. J. Millis, *Phys. Rev. Lett.* **99**, 146404 (2007).
- ³¹ J. Bauer and A. C. Hewson, *Phys. Rev. B* **81**, 235113 (2010).
- ³² R. Peierls, *Surprises in Theoretical Physics* (Princeton University Press, New Jersey, 1979).
- ³³ G. Beni, P. Pincus, and J. Kanamori, *Phys. Rev. B* **10**, 1896 (1974).
- ³⁴ H. Bakrim and C. Bourbonnais, *Phys. Rev. B* **76** (2007).
- ³⁵ Y. Takada and A. Chatterjee, *Phys. Rev. B* **67**, 081102 (2003).
- ³⁶ H. Fehske, A. P. Kampf, M. Sekania, and G. Wellein, *Eur. Phys. J. B* **31**, 11 (2003).
- ³⁷ M. Hohenadler and F. F. Assaad, *J. Phys.: Condens. Matter* **25**, 014005 (2013).
- ³⁸ A. Luther and V. J. Emery, *Phys. Rev. Lett.* **33**, 589 (1974).
- ³⁹ V. J. Emery, in *Highly conducting one-dimensional solids*, edited by J. T. Devreese (Plenum Press, New York, 1979), p. 247.
- ⁴⁰ J. Voit, *Eur. Phys. J. B* **5**, 505 (1998).
- ⁴¹ T. Giamarchi, *Quantum physics in one dimension* (Clarendon Press, Oxford, 2004).
- ⁴² R. Citro, E. Orignac, and T. Giamarchi, *Phys. Rev. B* **72**, 024434 (2005).
- ⁴³ M. Hohenadler, D. Neuber, W. von der Linden, G. Wellein, J. Loos, and H. Fehske, *Phys. Rev. B* **71**, 245111 (2005).
- ⁴⁴ M. Hohenadler, G. Hager, G. Wellein, and H. Fehske, *J. Phys.: Condens. Matter* **19**, 255202 (2007).
- ⁴⁵ J. Voit, *Rep. Prog. Phys.* **58**, 977 (1995).
- ⁴⁶ F. F. Assaad, *Phys. Rev. B* **78**, 155124 (2008).
- ⁴⁷ H. Fehske, G. Wellein, A. Weisse, F. Gohmann, H. Buttner, and A. R. Bishop, *Physica B* **312-313**, 562 (2002).
- ⁴⁸ A. N. Rubtsov, V. V. Savkin, and A. I. Lichtenstein, *Phys. Rev. B* **72**, 035122 (2005).
- ⁴⁹ M. Hohenadler, H. Fehske, and F. F. Assaad, *Phys. Rev. B* **83**, 115105 (2011).
- ⁵⁰ F. F. Assaad and T. C. Lang, *Phys. Rev. B* **76**, 035116 (2007).
- ⁵¹ E. Gull, A. J. Millis, A. I. Lichtenstein, A. N. Rubtsov, M. Troyer, and P. Werner, *Rev. Mod. Phys.* **83**, 349 (2011).
- ⁵² K. S. D. Beach, arXiv:0403055 (2004).
- ⁵³ L. Balents and M. P. A. Fisher, *Phys. Rev. B* **53**, 12133 (1996).
- ⁵⁴ M. Hohenadler, G. Wellein, A. R. Bishop, A. Alvermann, and H. Fehske, *Phys. Rev. B* **73**, 245120 (2006).
- ⁵⁵ C. E. Creffield, G. Sangiovanni, and M. Capone, *Eur. Phys. J. B* **44**, 175 (2005).
- ⁵⁶ S. Sykora, A. Hübsch, K. W. Becker, G. Wellein, and H. Fehske, *Phys. Rev. B* **71**, 045112 (2005).
- ⁵⁷ V. Meden, K. Schönhammer, and O. Gunnarsson, *Phys. Rev. B* **50**, 11179 (1994).
- ⁵⁸ R. T. Clay, A. W. Sandvik, and D. K. Campbell, *Phys. Rev. B* **59**, 4665 (1999).
- ⁵⁹ H. J. Schulz, *Phys. Rev. Lett.* **64**, 2831 (1990).
- ⁶⁰ K. Yonemitsu and M. Imada, *Phys. Rev. B* **54**, 2410 (1996).
- ⁶¹ F. H. L. Essler and A. M. Tsvelik, *Phys. Rev. Lett.* **88**, 096403 (2002).
- ⁶² J. Voit, L. Perfetti, F. Zwick, H. Berger, G. Margaritondo, G. Grüner, H. Höchst, and M. Grioni, *Science* **290**, 501 (2000).
- ⁶³ D. Sénéchal, D. Perez, and D. Plouffe, *Phys. Rev. B* **66**, 075129 (2002).